Three-Dimensional All Aspect Impact Angle Control Guidance Law with Field of View Constraint

Thesis to be submitted in partial fulfillment of the requirements for the degree

of

BTech in Aerospace Engineering

by

Aswin D Menon
21AE10044

Under the guidance of

Prof. Sikha Hota

AEROSPACE ENGINEERING

INDIAN INSTITUTE OF TECHNOLOGY KHARAGPUR

DECLARATION

I certify that

1. The work contained in this report has been done by me under the guidance of my supervisor.
2. The work has not been submitted to any other Institute for any degree or diploma.
3. I have conformed to the norms and guidelines given in the Ethical Code of Conduct of the Institute.
4. Whenever I have used materials (data, theoretical analysis, figures, and text) from other sources, I have given due credit to them by citing them in the text of the thesis and giving their details in the references. Further, I have taken permission from the copyright owners of the sources, whenever necessary.

Date: 27/04/2025 (Aswin D Menon)

Place: Kharagpur (21AE10044)

Department of Aerospace Engineering

Indian Institute of Technology, Kharagpur

India - 721302

CERTIFICATE

This is to certify that we have examined the thesis entitled **Three-Dimensional All Aspect Impact Angle Control Guidance Law with Field of View Constraint**, submitted by **Aswin D Menon** (Roll Number: **21AE10044**), an undergraduate student of **Department of Aerospace Engineering** in partial fulfillment for the award of degree of BTech in Aerospace Engineering. We hereby accord our approval of it as a study carried out and presented in a manner required for its acceptance in partial fulfillment for the Under Graduate Degree for which it has been submitted. The thesis has fulfilled all the requirements as per the regulations of the Institute and has reached the standard needed for submission.

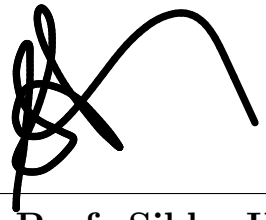

Prof. Sikha Hota

Department of Aerospace Engineering

Indian Institute of Technology, Kharagpur

Place: Kharagpur
Date: 27/04/2025

ACKNOWLEDGEMENTS

I sincerely acknowledge the support and guidance of Prof. Sikha Hota, Department of Aerospace Engineering, IIT Kharagpur, whose expertise and assistance were invaluable to the completion of this project thesis.

Aswin D Menon
IIT Kharagpur
Date: 27/04/2025

ABSTRACT

In this work, three novel three-dimensional (3D) impact angle control guidance (IACG) laws are developed targeting the objectives of achieving any arbitrary terminal impact directions while considering seeker field-of-view (FOV) constraints and ensuring a continuous lateral acceleration profile. The approach of all the three laws are similar. The 3D missile-target interception problem is decomposed into two planar engagements. Initially, a pure proportional navigation (PN) law is employed in the first plane to align the missile's velocity vector with the line-of-sight (LOS) to a virtual target. Subsequently, the engagement is transformed into a 2D problem on a second plane. For the 2-Staged PNG to TPG law, the TPG law is implemented on the second plane. For the 3-Staged PNG to Triangle TPG, the triangle TPG Law, which is a variation of the TPG Law, is implemented on the second plane. Finally, for the 3-Staged 3D IACG, a small variation of the two-stage time-varying biased proportional navigation (TVBPN) law governs the missile's approach towards the desired impact angle, on the second plane. A critical aspect of the design is the calculation of the virtual target's position to eliminate acceleration discontinuities during phase transitions. Extensive simulations are then conducted for all three laws. Furthermore, comparative simulations are done to validate the superiority of the proposed guidance law. It is then concluded that the proposed 3-staged 3D IACG law enables interception across all terminal conditions while satisfying FOV constraints and maintaining smooth acceleration profiles, thereby fulfilling the practical requirements for realistic missile engagements.

Contents

List of Figures

Chapter 1

Introduction

Missile guidance systems represent a critical area of research, encompassing the development and implementation of algorithms that steer a missile toward a designated target. The effectiveness of these guidance laws is paramount for ensuring accurate intercepts, minimizing collateral damage, and maximizing the destructive potential of the warhead. Effective guidance design must account for a multitude of factors, including target maneuvers, aerodynamic disturbances, and the missile's inherent kinematic constraints. Furthermore, practical limitations, such as restricted sensor fields-of-view and the need for smooth, achievable acceleration commands, introduce additional complexities.

In particular, achieving any desired impact angle plays a crucial role in maximizing warhead effectiveness and minimizing collateral damage. Since FOV (Field-of-View) constraints are inherent in any realistic seeker system, guidance laws are also required to ensure the target remains within the seeker's vision throughout the engagement. Moreover, discontinuous acceleration commands can induce excessive stress on the missile airframe. Therefore, a continuous acceleration profile is essential for practical implementation.

In recent years, quite a large number of studies have been conducted to design Impact Angle Control Guidance (IACG) laws for planar engagements. Ratnoo and Ghose (1) proposed a composite proportional navigation (PN)-based guidance law by combining an orientation phase with classical PN in the terminal phase to achieve any desired impact angle. This study was extended in (2) to address the interception of non-stationary, non-maneuvering targets. FOV constraints were satisfied in addition to achieving all possible impact angles in a two-staged PN guidance (PNG) law in (3). The same objectives were achieved with a lesser control effort using a three-staged PN guidance law by Ranjan et al. (4). Since these guidance laws are multi-stepped-PN-based, their missile lateral acceleration profiles are discontinuous, or have abrupt jumps. Park et al. (5, 6) designed a

two-staged biased proportional navigation guidance (BPNG) law that considers FOV and lateral acceleration limits. An energy-optimal impact angle control guidance law that explicitly incorporates FOV constraints for missiles equipped with strap-down seekers was presented in (7). Lee et al. (8) proposed a time-to-go polynomial guidance (TPG) law while satisfying both terminal acceleration and seeker FOV constraints, where the acceleration command was formulated as a polynomial function of time-to-go. A time-varying two-staged BPNG law was designed by Yang et al. (9) to achieve all possible impact angles while maintaining an FOV constraint. As all the guidance laws mentioned till now are for 2D engagement scenarios, their real-life applicability is limited.

In order to address the complexities of realistic missile-target interaction, the more recent research has extended impact angle control guidance into three-dimensional frameworks. Erer and Tekin (10) proposed two guidance laws that extend biased PN to 3D engagement by rotating either the LOS (Line of Sight) or velocity vector toward the desired terminal direction. A quaternion based guidance law that expands a 2D BPNG law into 3D by incorporating quaternion rotation between the missile's current velocity and the desired impact direction was proposed in (11). Wing et al. (12) presented a nonlinear guidance law that enables simultaneous control of impact angle and impact time in two stages–a sliding-mode-based IACG first and then a PNG later. Another nonlinear guidance law, proposed in (13), ensures interception within a predefined convergence time, using a sliding mode control framework and a predefined-time stability theory. Nanavati et al. (14) proposed yet another nonlinear guidance law that uses a finite-time state-dependent Riccati equation and a lead-angle-based formulation. Zhou et al., in (15), proposed an IACG by decomposing the trajectory into two independently designed nominal curves– an elliptical path in the vertical plane and a Bézier curve in the lateral plane. However, these 3D engagement studies do not consider the FOV constraints of the seeker.

In real-world conditions, the FOV is generally limited due to physical constraints. Hence, the FOV constraints should be considered in guidance laws to ensure that the missile can stay within its tracking limits and successfully intercept the target. Duvvuru et al. (16) proposed a guidance law that satisfies the terminal impact angle and the FOV constraints while maximizing the terminal speed and minimizing flight time, using an extended form of the Generalized Model Predictive Static Programming technique. In (17), a guidance law was proposed that enforces prescribed performance and FOV constraints by shaping LOS angle errors through a range-dependent prescribed performance function. A predefined-time IACG law was introduced in (18) that uses a novel predefined-time error dynamic

tailored for second-order systems and auxiliary functions to prevent FOV violations. Wang et al. (19) proposed an FOV-constrained guidance law that combines a PN term with a bias component shaped by a nonlinear error dynamic for speed-varying missiles. Another FOV-constrained guidance law (20) that constructs range profiles as cubic polynomials of LOS angles was proposed for speed-varying missiles. Hu et al. (21) proposed a guidance law that achieves both impact angle and seeker FOV constraints using polynomial shaping of LOS angles in pitch and yaw, formulated as cubic polynomials of relative range. A similar study was conducted in (22). Ghosh et al., in (23), proposed a composite PN based guidance law ($\mu\alpha$CIG3D) that enables UAVs to approach a stationary target from any arbitrary direction in 3D space while accounting for FOV limitations. This law, however, causes multiple jumps in the lateral acceleration profile. None of the 3D engagement IACG laws discussed above could simultaneously address FOV constraints and achieve any terminal direction.

Following the observations above, the goal of this study is to design a 3D Impact Angle Control Guidance (IACG) law, for stationary targets, that can achieve any desired terminal missile direction while considering the seeker's Field-of-View (FOV) limits. In this study, the 3D missile interception problem is decomposed into two planes. Initially, a pure PNG law is employed in the first plane, containing the initial velocity vector and the initial Line-of-Sight (LOS), towards a virtual target on the initial LOS to align the missile's velocity vector in line with the LOS. Subsequently, the engagement in the second plane, containing the current velocity vector and the impact angle vector, is reduced to a 2D problem. An FOV-constrained 2D IACG law capable of achieving any desired impact angle is then implemented in this second plane. The position of the virtual target in the initial stage should ideally be such that there is no discontinuity in the magnitude of lateral acceleration during phase transition.

Chapter 2

Problem Statement

The Three-Dimensional Missile-Target engagement geometry is shown in Figure 2.1. M and T denote the initial positions of the missile and target, respectively. (X, Y, Z) represents the inertial coordinate system with origin at O. As discussed in the introduction, in this study, the engagement is carried out in two planes. T' is the location of the virtual target considered in the first stage. The missile trajectory switches to the second plane when the missile velocity aligns with the LOS, at P_{12}. e_{LOS_1} represents the unit vector along the initial LOS (Line of sight) vector. The initial velocity of the missile is along the unit vector e_{m_0}. e_{LOS_2} is the unit vector along the LOS at the beginning of the second stage. e_{m_f} denotes the unit impact vector, which is the desired direction of missile interception. The cross operator $(\times)$ represents the vector cross product. The normals to the two planes, as shown in Figure 2.1, are:

$$e_{N_1} = e_{LOS_1} \times e_{m_0}; \quad e_{N_2} = e_{m_f} \times e_{LOS_2} \tag{2.1}$$

For each plane, separate coordinate axes are set. The origin of the first plane is set at the initial position, M, of the missile. e_{LOS_1} is set as the X-axis and $(e_{N_1} \times e_{LOS_1})$ is set as the Y-axis. For the second plane, e_{LOS_2} and $(e_{N_2} \times e_{LOS_2})$ are set as X-axis and Y-axis respectively, with the switching point P_1 as the origin.

In 3D space, the attitude of a vector can be represented by 2 angles: Azimuth angle (ψ) and Elevation angle (θ). ψ varies from $-180°$ to $180°$ and θ varies from $-90°$ to $90°$. For example, as shown in Figure 2.2, consider a vector $\vec{A}$, having projections a_x, a_y, and a_z along X, Y, and Z axes, respectively. Then, the associated angles can be given by:

$$\psi = \tan^{-1}\left(\frac{a_y}{a_x}\right) \tag{2.2}$$

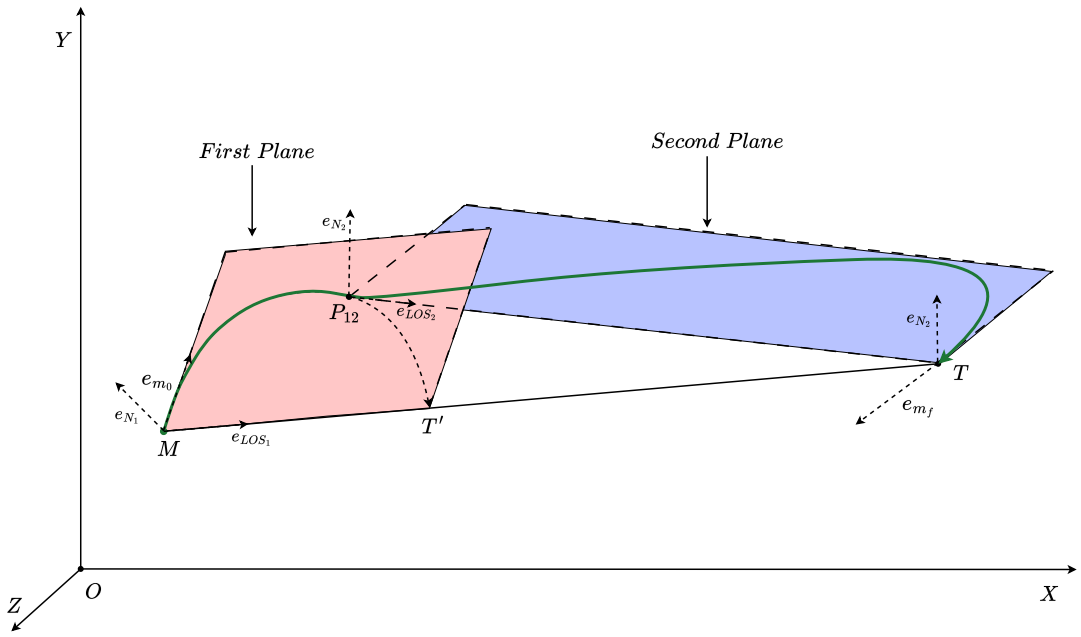

Figure 2.1: 3D Engagement Scenario

$$\theta = \tan^{-1}\left(\frac{a_z}{\sqrt{a_x^2 + a_y^2}}\right) \tag{2.3}$$

Conversely, for a given vector $\vec{A}$ and angles ψ and θ, the components a_x, a_y and a_z can be given by:

$$a_x = |\vec{A}|cos(\theta)cos(\psi) \tag{2.4}$$

$$a_y = |\vec{A}|cos(\theta)sin(\psi) \tag{2.5}$$

$$a_z = |\vec{A}|sin(\theta) \tag{2.6}$$

Since the interception is achieved as a combination of two 2D engagement problems, the 2D engagement geometry and kinematics has to be discussed. In Figure 2.3, M and T denote the positions of the missile and target, respectively. (X, Y) represents the inertial coordinate system with origin at O. M' denotes the position of the missile at some time during the engagement. Subscripts '0' and 'f' denote initial and final conditions, respectively. The

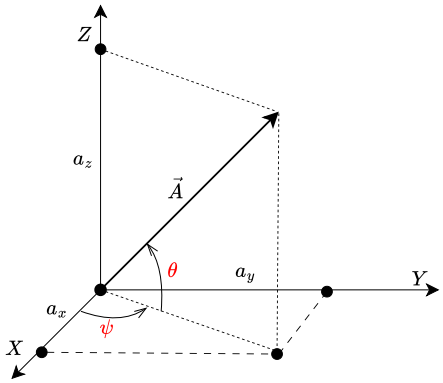

Figure 2.2: 3D Angles

velocity of the missile is represented by the vector $\vec{V}$, of magnitude V. r denotes the relative range or the length of LOS. The flight path angle, γ, is the angle the missile's velocity makes with the horizontal axis. σ denotes the look angle, which is the angle between the missile's velocity vector and the LOS. The LOS angle, λ, is the angle made by the LOS with the horizontal. And, a_m is the lateral acceleration of the missile. The dot operator represents the derivative of a variable with respect to time. The kinematics of the engagement for a constant-speed missile towards a stationary target are then be given by:

$$\dot{r} = -V\cos(\gamma - \lambda) \tag{2.7}$$

$$\dot{\lambda} = \frac{-V\sin(\gamma - \lambda)}{r} \tag{2.8}$$

$$\sigma = \gamma - \lambda \tag{2.9}$$

$$\dot{\gamma} = \frac{a_M}{V} \tag{2.10}$$

For a pure PN guidance law, the guidance command, a_M, and the time rate of change of flight path angle, $\dot{\gamma}$, are given by:

$$a_M = NV\dot{\lambda}; \quad \dot{\gamma} = N\dot{\lambda} \tag{2.11}$$

where N is the navigation gain, V is the speed of the missile, and $\dot{\lambda}$ is the time derivative of the LOS angle (λ). $\dot{\gamma}$ is the time rate of change of the flight path angle (γ).

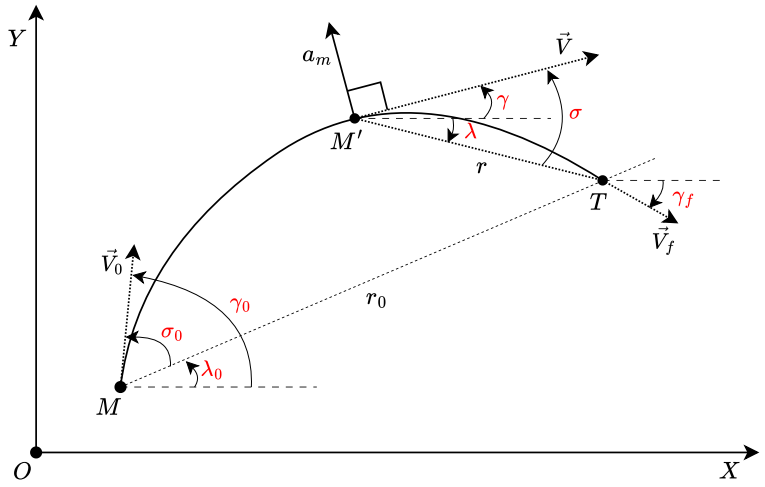

Figure 2.3: 2D Engagement Geometry

The guidance command, a_M, and the time rate of change of flight path angle, $\dot{\gamma}$, of a biased PN guidance law are formulated as:

$$a_m = NV\dot{\lambda} + Vb; \quad \dot{\gamma} = N\dot{\lambda} + b \tag{2.12}$$

where N is the navigation gain and b is the bias term, which may be used to improve the guidance law's performance. Integrating $\dot{\gamma}$ with respect to time, using some initial conditions, gives:

$$\gamma(t) - \gamma_0 = N(\lambda(t) - \lambda_0) + \int_0^t b\,dt \tag{2.13}$$

where $\int_0^t b\,dt$ is the integral value of bias, B. If a certain terminal impact angle (γ_f) is desired, the integral of the bias term is expected to reach a certain value, which can be found by substituting $t = t_f$ in (2.13). We then get:

$$\gamma_f - \gamma_0 = N(\lambda_f - \lambda_0) + \int_0^{t_f} b\,dt \tag{2.14}$$

At the terminal conditions, $\gamma_f = \lambda_f$. Hence, the expected integral of bias or the reference integral of bias, B_{ref}, is given by:

$$B_{ref} = \int_0^{t_f} b\,dt = (1-N)\gamma_f + N\lambda_0 - \gamma_0 \tag{2.15}$$

Chapter 3

2-Staged PNG to TPG Law

3.1 Overview

The objective, as mentioned in the introduction, is to build an FOV-constrained 3D impact angle control guidance (IACG) law that can achieve any terminal impact direction, all while maintaining a continuous acceleration profile. The methodology of this problem, as shown in Figure 2.1, is to carry out the engagement in two planes. Engagement on the first plane is to ensure that the missile velocity aligns with the LOS vector, which then essentially makes the rest of the engagement a 2D problem. Here, the time-to-go polynomial guidance (TPG) law (8) is implemented on the second plane for the desired interception.

3.2 Review of the TPG law

The TPG formulates the guidance command as a polynomial function of time-to-go, with coefficients determined to satisfy specified terminal conditions. A systematic method is presented for determining guidance gains that respect practical limitations, including actuator saturation and seeker field-of-view (FOV) constraints. A time-to-go estimation method for TPG implementation is also discussed. Time-to-go, in other words, is the time remaining till interception. For the TPG, the acceleration command is given by:

$$a_M(t) = -\frac{V_M}{t_{go}}\left[-(m+2)(n+2)\lambda(t) + (m+n+3)\gamma_M(t) + (m+1)(n+1)\gamma_f\right] \tag{3.1}$$

where t_{go} is the time-to-go and γ_f is the desired impact angle. m and n are the TPG guidance gains, which are to be chosen according to the requirements of FOV and acceleration. The λ and γ can be measured directly from the built in seeker and internal navigation

system respectively. But the time-to-go t_{go} has to be estimated. A TPG-mn guidance law represents that the guidance gains are m and n.

The Time-to-go t_{go}, which cannot be measured using sensors, is given by:

$$t_{go} = \frac{S(t)}{V_M} = \frac{R}{V_M}\left\{1 + P_1\left[\left(\frac{1}{2}(\gamma_M - \gamma_f) - P_2(\lambda - \gamma_f)\right)^2 + P_3(\gamma_M - \gamma_f)^2\right] - \frac{1}{2}(\lambda - \gamma_f)^2\right\} \tag{3.2}$$

where $S(t)$ is the estimated distance to cover between t (initial time) and t_f (final time). $S(t)$ is given by:

$$S(t) = R\left\{1 + P_1\left[\left(\frac{1}{2}\bar{\gamma}_M - P_2\bar{\lambda}\right)^2 + P_3\bar{\gamma}_M^2\right] - \frac{1}{2}\bar{\lambda}^2\right\} \tag{3.3}$$

where:

$$P_1 = \frac{1}{(2m+3)(2n+3)(m+n+3)} \tag{3.4}$$

$$P_2 = (m+2)(n+2) \tag{3.5}$$

$$P_3 = \left(m + \frac{3}{2}\right)\left(n + \frac{3}{2}\right) \tag{3.6}$$

The TPG ensures that the terminal acceleration constraints, of zero acceleration and zero jerk, are obeyed. But, the drawback is that this law cannot achieve all impact angles for gain values of $m = 2$ and $n = 3$. It is only for low gains like $m = 1.001$ and $n = 2.001$ that the law will be able to achieve all impact angles. Only when the gains are above 1 are the terminal acceleration constraints obeyed.

3.3 Design of the 2-Staged PNG to TPG Law

The engagement consists of two stages: the first stage on the first plane and the second stage on the second plane. For the planes of engagement, as seen in Figure 2.1, the coordinates are given by:

$$X_1 = e_{LOS_1}; \quad Y_1 = e_{N_1} \times e_{LOS_1} \tag{3.7}$$

$$X_2 = e_{LOS_2}; \quad Y_2 = e_{N_2} \times e_{LOS_2} \tag{3.8}$$

where (X_1, Y_1) and (X_2, Y_2) represent the coordinates of the first and the second plane, respectively. The speed of the missile, V, remains constant throughout the engagement. For the engagement on the first plane, in order to align the missile's velocity vector with the LOS, a pure PNG of navigation gain $N = 2$ is used. In this initial stage, the missile is engaged towards a virtual target that lies on the initial LOS. The position of the target is at the k^{th} fraction of the initial LOS. As the gain of the PNG is 2, the missile follows a circular trajectory. The acceleration and the time rate of change of flight path angle in the first plane is given by:

$$a_{M_1} = 2V\dot{\lambda_1}; \quad \dot{\gamma_1} = 2\dot{\lambda_1} \tag{3.9}$$

where the subscript '1' represents the variables with respect to the first-plane coordinate system (X_1, Y_1) (equation (3.7)). The λ_1, hence, is the LOS to the virtual target at T'. V is the speed of the missile. The look angle rate becomes:

$$\dot{\sigma_1} = \dot{\gamma_1} - \dot{\lambda_1} = \dot{\lambda_1} \tag{3.10}$$

This stage continues until the flight path angle equals the LOS angle, which is a condition for the missile velocity being aligned with the LOS. Thus, the switching to the second stage occurs when:

$$\gamma = \lambda \tag{3.11}$$

where γ and λ are the angles in the 3D frame (X, Y, Z). The initial conditions of the first stage, as the X axis is taken along the direction of LOS, e_{LOS_1}, are:

$$\sigma_{1_0} = \gamma_{1_0}; \quad \lambda_{1_0} = 0 \tag{3.12}$$

where the subscript '0' denotes the initial condition.

For the second stage of the engagement, a TPG of $n = 1.001$ and $m = 2.001$ is used. When the gains are such, the missile can achieve all 2D impact angles. Since the second stage of the engagement is essentially a 2D problem, this TPG law would satisfy the requirements. The acceleration command in the second plane is hence given by:

$$a_{M_2}(t) = -\frac{V}{t_{go}}\left[-(m+2)(n+2)\lambda_2(t) + (m+n+3)\gamma_2(t) + (m+1)(n+1)\gamma_{2_f}\right] \tag{3.13}$$

$$a_{M_2}(t) = -\frac{V}{t_{go}}\left[-12.007\lambda_2(t) + 6.002\gamma_2(t) + 6.005\gamma_{2_f}\right] \tag{3.14}$$

where the subscript '2' represents the variables with respect to the second-plane coordinate system (X_2, Y_2) (equation (3.7)). Thus, the γ_{2_f} is the required final impact angle in the second plane.

Since initially, the velocity vector is aligned with the LOS and the X axis is along the direction of LOS, e_{LOS_2}, the initial conditions are:

$$\sigma_{2_0} = 0; \quad \lambda_{2_0} = 0; \quad \gamma_{2_0} = 0 \tag{3.15}$$

3.4 Simulations

Simulations were done in MATLAB for both the TPG law and the novel 2-Staged PNG to TPG Law, for a constant-speed missile and a stationary target.

3.4.1 The TPG guidance law

The TPG law was simulated for a constant-speed missile at a speed of 200 m/s. As mentioned, m is taken as 1.001 and n is taken as 2.001. The missile was initially at (0.0) and the stationary target was at $(4000, 0)$. The initial missile flight path angle was 30°. The simulations were carried out for terminal impact angles of 0°, −30°, −90°, −120°, −150° and −180°. The plots of the obtained results are shown in Figure 3.1.

3.4.2 The 2-Staged PNG to TPG Law

Simulations of the novel 2-Staged PNG to TPG Law, designed as a 3D extension to the TPG law, were then conducted for a constant-speed missile at a speed of 50 m/s. The initial location of the missile was $(0, 0, 0)$ and the target location was $(2500, 2500, 2500)$. The initial velocity was along the vector $(-1, 1, 1)$. For the TPG used in the second plane, the gains m and n were taken as 1.001 and 2.001, respectively. The impact conditions of the form (Azimuth angle, Elevation Angle) were taken as $(-45°, -45°)$, $(-60°, -30°)$, $(-30°, -60°)$, $(-90°, -45°)$ and $(-179°, -75°)$. The obtained plots are shown in Figure 3.2.

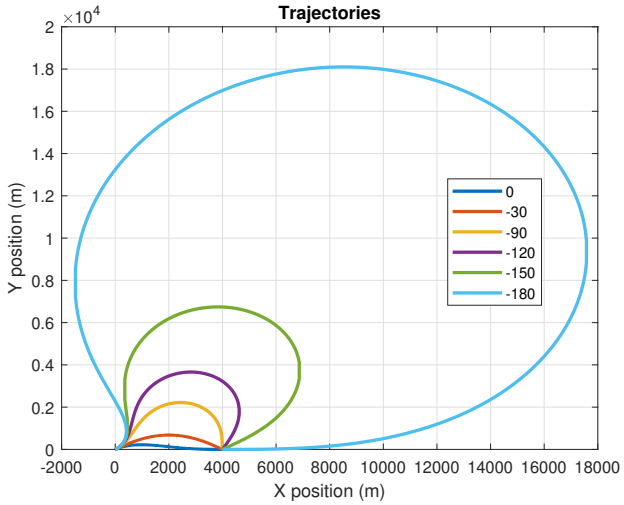

(a)

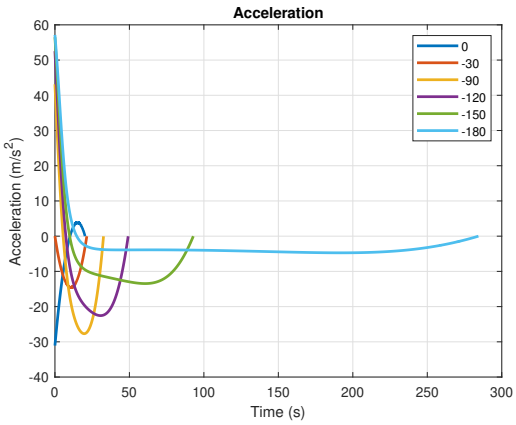

(b)

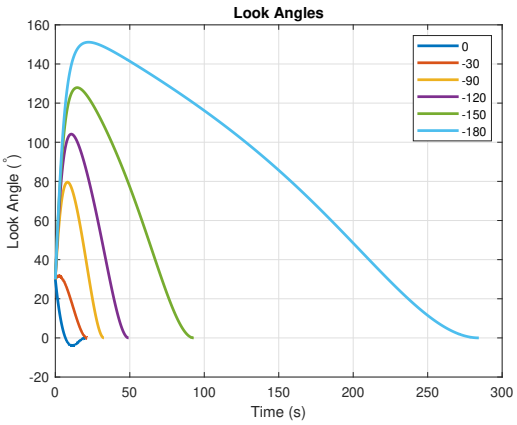

(c)

Figure 3.1: Simulation results of 2D TPG Law

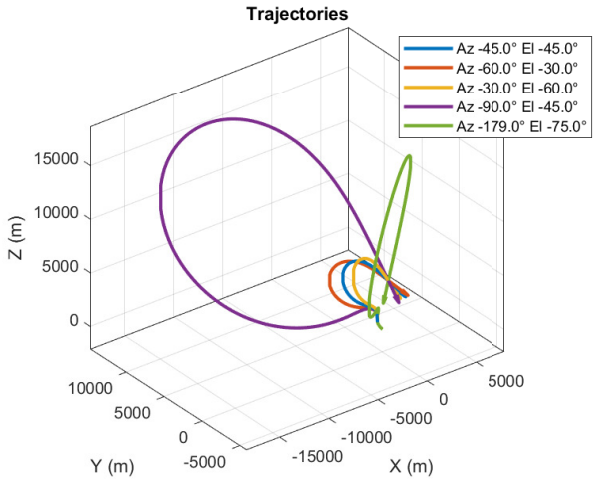

(a)

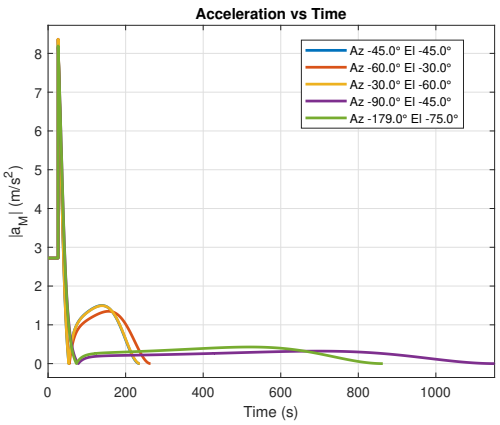

(b)

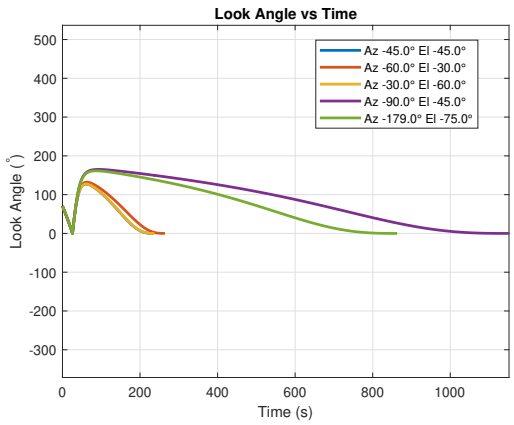

(c)

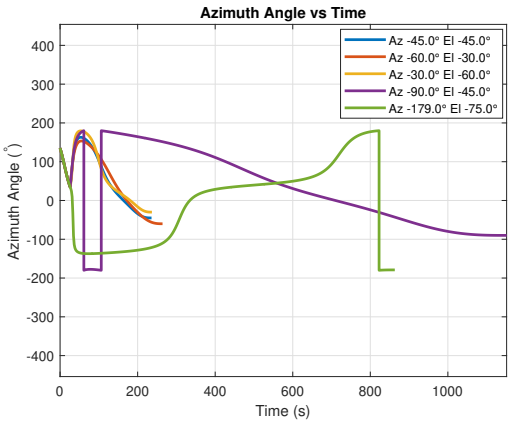

(d)

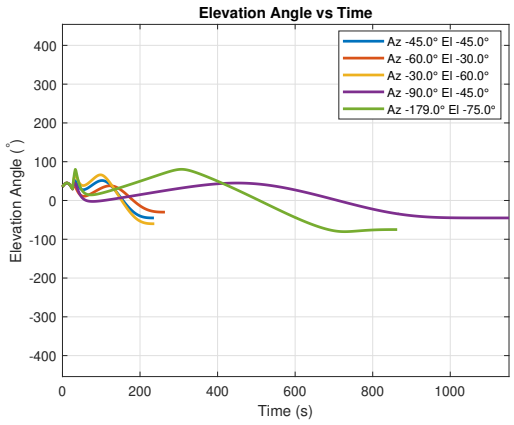

(e)

Figure 3.2: Simulation results of 2-Staged PNG to TPG Law

Chapter 4

3-Staged PNG to Triangle TPG Law

4.1 Overview

This law attempts to achieve the objectives by performing the interception in two stages or planes, as shown in 2.1, just as it was for the 2-Staged PNG to TPG. The engagement in the second plane essentially becomes a 2D problem. Here, a variation of the TPG law (8) is used on the second plane for successful interception.

4.2 Triangle TPG Law

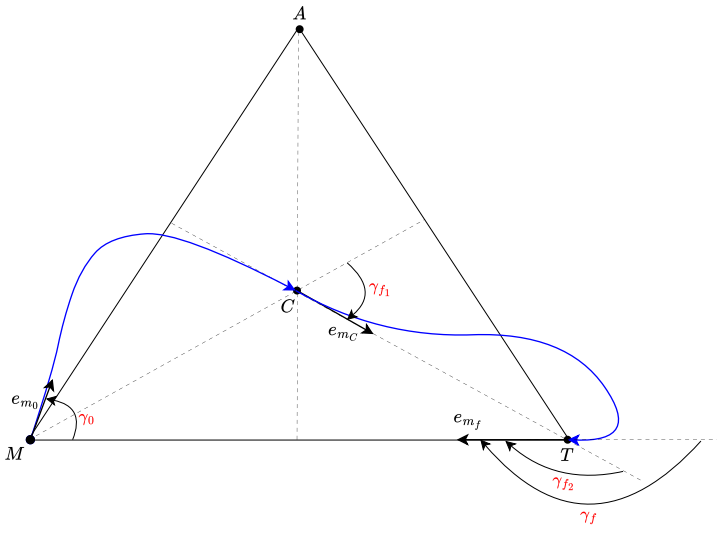

Figure 4.1: Triangle TPG - Extreme Case

A variation of the already existing TPG law was designed to achieve all impact angles in the second plane of engagement, without selecting low TPG gain values. This is done by decomposing the 2D problem into two stages, as seen in Figure 4.1. The missile is found to achieve all negative impact angles of $0°$to$-120°$ for TPG gains of $m = 2$ and $n = 3$. So, to extend this range beyond $-120°$, an equilateral triangle is initially built with the initial LOS as one of the sides. Now, the centroid of the circle is taken as the virtual target for the first phase. For the worst case ($\gamma_f = -180°$), the first impact angle, γ_{f_1}, at C is taken as $-30°$, and then the second impact angle, γ_{f_2}, for the second phase is taken as $-120°$. The TPG gains for both phases are taken as $m = 2$ and $n = 3$. The initial missile flight path angle is taken as γ_0. The missile can achieve all impact angles in the negative spectrum with this method. e_{m_0}, e_{m_C}, and e_{m_f} denote the unit vectors along the initial velocity, the impact direction at the centroid, and the final impact direction, respectively.

This variation is used only when the magnitude of the final impact angle is more than $120°$. Otherwise, the normal TPG is used. For cases between $-120°$ and $-180°$, the mechanism remains the same as that for the worst case, except that the impact angle in the second phase changes. The impact angles would then be related by:

$$\gamma_{f_1} + \gamma_{f_2} = \gamma_f; \quad -\frac{\pi}{6} + \gamma_{f_2} = \gamma_f \tag{4.1}$$

Hence, the acceleration commands for the first and second phases become:

$$a_{M_1} = -\frac{V_M}{t_{go}} \left[-(m+2)(n+2)\lambda_1 + (m+n+3)\gamma_1 - \frac{(m+1)(n+1)\pi}{6} \right] \tag{4.2}$$

$$a_{M_1} = -\frac{V_M}{t_{go}} \left[-20\lambda_1 + 8\gamma_1 - 2\pi \right] \tag{4.3}$$

$$a_{M_2} = -\frac{V_M}{t_{go}} \left[-(m+2)(n+2)\lambda_2 + (m+n+3)\gamma_2 + (m+1)(n+1)\gamma_{f_2} \right] \tag{4.4}$$

$$a_{M_2} = -\frac{V_M}{t_{go}} \left[-20\lambda_2 + 8\gamma_2 + 12\gamma_{f_2} \right] \tag{4.5}$$

where '1' and '2' are the subscripts for the first and second phase variables, respectively. The t_{go} can be calculated using the equations (3.2), (3.3), (3.4), (3.5), and (3.6).

4.3 Design of the 3-Staged PNG to Triangle TPG Law

For this law, the engagement consists of three stages: the first stage on the first plane and the second and third stages on the second plane. For the planes of engagement, as seen in Figure 2.1, the coordinates are given by:

$$X_1 = e_{LOS_1}; \quad Y_1 = e_{N_1} \times e_{LOS_1} \tag{4.6}$$

$$X_2 = e_{LOS_2}; \quad Y_2 = e_{N_2} \times e_{LOS_2} \tag{4.7}$$

where (X_1, Y_1) and (X_2, Y_2) represent the coordinates of the first and the second plane, respectively. The speed of the missile, V, remains constant throughout the engagement. For the engagement on the first plane, in order to align the missile's velocity vector with the LOS, a pure PNG of navigation gain $N = 2$ is used. In this initial stage, the missile is engaged towards a virtual target that lies on the initial LOS. The position of the target is at the k^{th} fraction of the initial LOS. As the gain of the PNG is 2, the missile follows a circular trajectory. The acceleration and the time rate of change of flight path angle in the first plane is given by:

$$a_{M_1} = 2V\dot{\lambda_1}; \quad \dot{\gamma_1} = 2\dot{\lambda_1} \tag{4.8}$$

where the subscript '1' represents the variables with respect to the first-plane coordinate system (X_1, Y_1) (equation (3.7)). The λ_1, hence, is the LOS to the virtual target at T'. V is the speed of the missile. The look angle rate becomes:

$$\dot{\sigma_1} = \dot{\gamma_1} - \dot{\lambda_1} = \dot{\lambda_1} \tag{4.9}$$

This stage continues until the flight path angle equals the LOS angle, which is a condition for the missile velocity being aligned with the LOS. Thus, the switching to the second stage occurs when:

$$\gamma = \lambda \tag{4.10}$$

where γ and λ are the angles in the 3D frame (X, Y, Z). The initial conditions of the first stage, as the X axis is taken along the direction of LOS, e_{LOS_1}, are:

$$\sigma_{1_0} = \gamma_{1_0}; \quad \lambda_{1_0} = 0 \tag{4.11}$$

where the subscript '0' denotes the initial condition.

For the second plane, the triangle TPG law is used. As discussed before, the engagement in the second plane will consist of two phases if the magnitude of the terminal impact angle is 120°. The initial phase guides the missile to a virtual target located at the centroid of the equilateral triangle with the initial LOS as its base. From the centroid C, the missile is then guided to the target to satisfy the requirements successfully. The TPG gains for both phases are taken as $m = 2$ and $n = 3$. When the magnitude of the terminal impact angle is less than 120°, the TPG of $m = 2$ and $n = 3$ is used. All the impact angles can be achieved using this method for the second plane.

Hence, the acceleration commands, from equations (4.1), (4.2), (4.3), and (4.4), are given by:

$$a_M = \begin{cases} \left\{ a_{M_2} = -\frac{V_M}{t_{go}} \left[-20\lambda_2 + 8\gamma_2 + 12\gamma_f \right], \right. & \textit{if } \ |\gamma_f| < 120^\circ \\ \begin{cases} a_{M_2} = -\frac{V_M}{t_{go}} \left[-20\lambda_2 + 8\gamma_1 - 2\pi \right], & (M \text{ to } C) \\ a_{M_3} = -\frac{V_M}{t_{go}} \left[-20\lambda_3 + 8\gamma_3 + 12\gamma_{f_2} \right], & (C \text{ to } T) \end{cases} & \textit{if } \ |\gamma_f| \geq 120^\circ \end{cases} \tag{4.12}$$

where the subscripts '2' and '3' represent the variables in the second and third stages, respectively. M, C, and T denote the initial position of the missile, the centroid position of the equilateral triangle, and the target position. γ_{f_2} is the impact angle in the third phase and is given by:

$$\gamma_{f_2} = \gamma_f + \frac{\pi}{6} \tag{4.13}$$

The engagement in the second plane happens in the (X_2, Y_2) coordinates (equation 4.7). Since initially, the velocity vector is aligned with the LOS and the X axis is along the direction of LOS, e_{LOS_2}, the initial conditions are:

$$\sigma_{2_0} = 0; \quad \lambda_{2_0} = 0; \quad \gamma_{2_0} = 0 \tag{4.14}$$

4.4 Simulations

Both the variation of TPG law and the novel 3-Staged PNG to Triangle TPG Law were simulated in the MATLAB environment, for a constant-speed missile and a stationary target.

4.4.1 The variation of TPG guidance law

The variation of the TPG law was simulated for a constant-speed missile at a speed of 200 m/s. As mentioned earlier, m is taken as 2 and n is taken as 3. The missile was initially at (0.0) and the stationary target was at $(4000, 0)$. The initial missile flight path angle was $0°$, as was required for the second plane. The simulations were carried out for terminal impact angles of $0°$, $-30°$, $-90°$, $-120°$, $-150°$, and $-180°$. The plots of the obtained results are shown in Figure 4.2.

4.4.2 The 3-Staged PNG to Triangle TPG Law

Simulations of the novel 3-Staged PNG to TPG Law, designed as a 3D extension to the variation of the TPG law, were then conducted for a constant-speed missile at a speed of 50 m/s. The initial location of the missile was $(0, 0, 0)$ and the target location was $(2500, 2500, 2500)$. The initial velocity was along the vector $(-1, 1, 1)$. For the TPG used in the second plane, the gains m and n were taken as 2 and 3, respectively. The impact conditions of the form (Azimuth angle, Elevation Angle) were taken as $(-45°, -45°)$, $(-60°, -30°)$, $(-30°, -60°)$, $(-90°, -45°)$ and $(-179°, -75°)$. The obtained plots are shown in Figure 4.3.

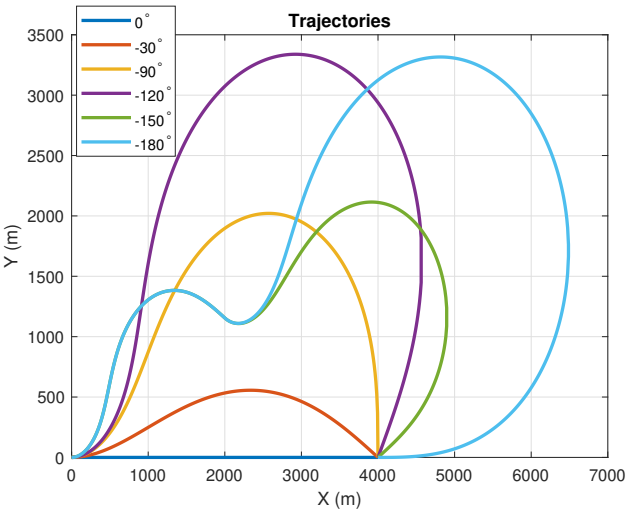

(a)

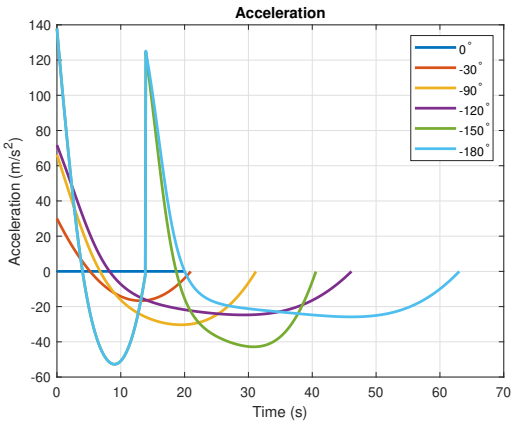

(b)

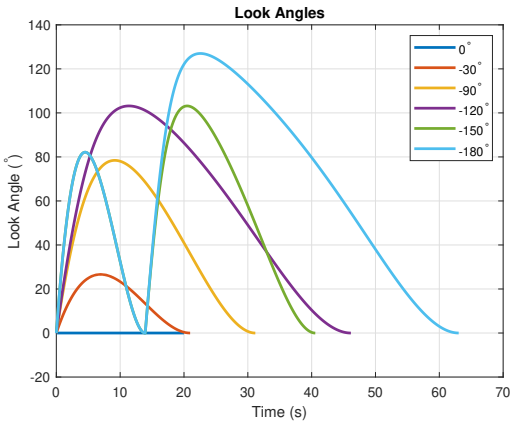

(c)

Figure 4.2: Simulation results of Triangle TPG Law

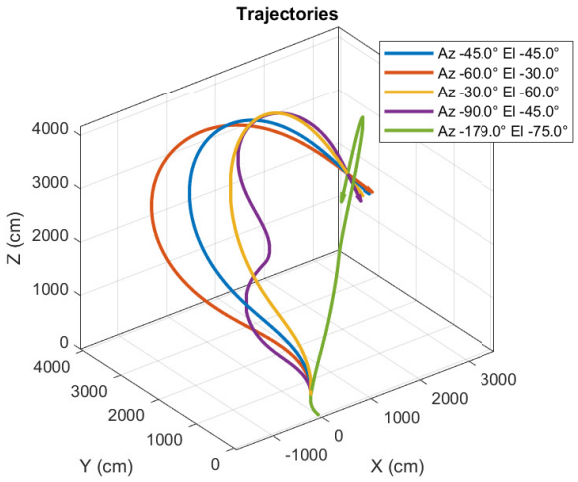

(a)

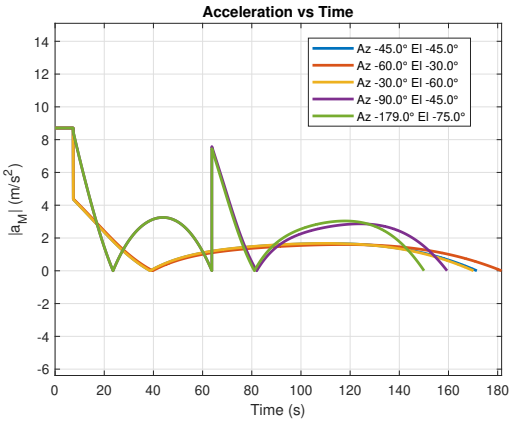

(b)

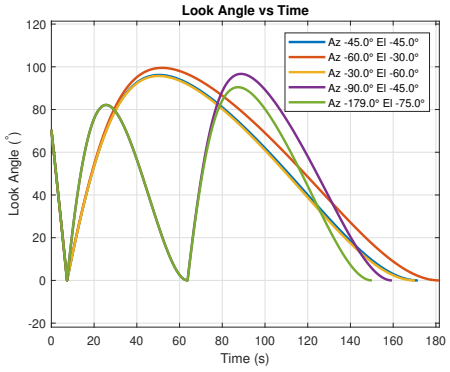

(c)

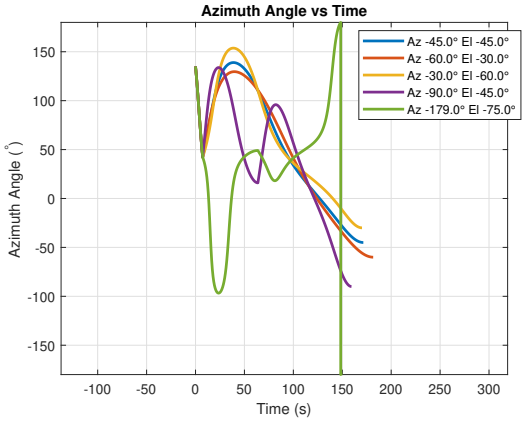

(d)

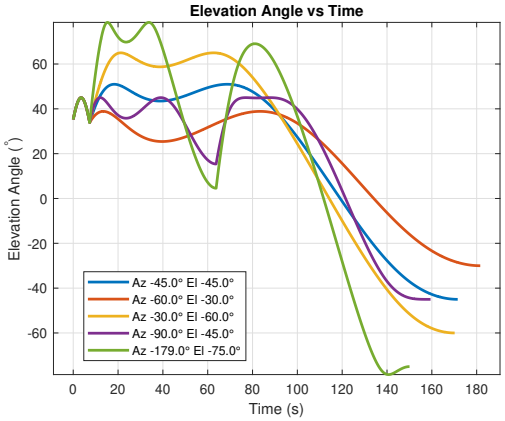

(e)

Figure 4.3: Simulation results of 3-Staged PNG to Triangle TPG Law

Chapter 5

3-Staged 3D IACG Law

5.1 Overview

The FOV-constrained 3D IACG designed in this chapter will be able to achieve all terminal impact directions while maintaining a continuous acceleration profile. As discussed in the introduction, the first stage of the law, on the first plane, ensures that the missile's velocity aligns with the LOS. When the velocity is in line with the LOS, achieving all possible impact directions essentially becomes a 2D problem for the engagement on the second plane. To eliminate a jump in the acceleration profile during phase transition, the position of the virtual target of the first phase is chosen such that the terminal acceleration of the first phase equals the initial acceleration of the second phase. The overall engagement contains three stages: the first stage on the first plane and the second and third stages on the second plane.

5.2 Review of the TVBPN Guidance Law

For the second plane of the engagement, a 2D FOV-constrained IACG law, that can achieve all impact angles, should be implemented. Time-Varying Biased Proportional Navigation (TVBPN) guidance law, discussed in (9), satisfies these requirements. In this study, the engagement is carried out in two phases, by two different time-varying biases. A switching logic is used to transition between the two phases. For the initial phase, the bias term, b_1, is given by:

$$b_1 = (1 - N)\dot{\lambda} + \frac{1}{\tau_1}(\sigma_{\max} - \sigma) \tag{5.1}$$

where σ_{max} is the maximum allowed look angle and τ_1 is the time constant of convergence of σ to σ_{max}. The acceleration command, as of equation (2.12(a)), then becomes:

$$a_m = V\dot{\lambda} + \frac{V}{\tau_1}(\sigma_{\max} - \sigma) \tag{5.2}$$

The second stage is designed for converging B to B_{ref}, as discussed in the previous section. For the same, the second-phase bias, b_2, is given by:

$$b_2 = \dot{B}(t) = \frac{B_{\text{ref}} - B(t)}{\tau_2} \tag{5.3}$$

where τ_2 is the time constant of convergence of B to B_{ref}. Solving this linear differential equation then gives:

$$B(t) = \frac{(B_{\text{ref}} - B(t_s))\exp\left(-\frac{t-t_s}{\tau_2}\right)}{\tau_2} \tag{5.4}$$

where t_s is the phase-switching time and $B(t_s)$ is the integral value of bias at the switching instant. Hence, the acceleration, according to equation (2.12(a)), becomes:

$$a_M = N\dot{\lambda} + \frac{B_{\text{ref}} - B(t)}{\tau_2} \tag{5.5}$$

In the initial phase, the bias term, b_1, increases until the look angle, σ, reaches the maximum allowed value, σ_{max}. The second phase bias, b_2, decreases to zero as the integral of bias, B, converges to the required value, B_{ref}. The switching criteria can be expressed as:

$$b = \begin{cases} b_1, & |b_1| < |b_2| \\ b_2, & |b_1| \geq |b_2| \end{cases} \tag{5.6}$$

5.3 Design of the 3-staged 3D IACG law

For the planes of engagement, as seen in Figure 2.1, the coordinates are given by:

$$X_1 = e_{LOS_1}; \quad Y_1 = e_{N_1} \times e_{LOS_1} \tag{5.7}$$

$$X_2 = e_{LOS_2}; \quad Y_2 = e_{N_2} \times e_{LOS_2} \tag{5.8}$$

where (X_1, Y_1) and (X_2, Y_2) represent the coordinates of the first and the second plane, respectively.

The speed of the missile remains constant throughout the engagement. The guidance command is given only as lateral acceleration. For the engagement on the first plane, in

order to align the missile's velocity vector with the LOS, a pure PNG of navigation gain $N = 2$ is used. In this initial stage, the missile is engaged towards a virtual target that lies on the initial LOS. The position of the virtual target has to be calculated such that there is no discontinuity in the lateral acceleration when the engagement transitions from the first stage to the second. This calculation will be discussed later. As a pure PNG law of $N = 2$ forces the missile to follow a circular trajectory, the acceleration remains constant. This makes the calculation of the virtual point much easier. The guidance command and the time rate of change of the flight path angle of the missile in the first stage, on the first plane, are then given by:

$$a_{M_1} = 2V\dot{\lambda_1}; \quad \dot{\gamma_1} = 2\dot{\lambda_1} \tag{5.9}$$

where the subscript '1' represents the variables with respect to the first-plane coordinate system (X_1, Y_1) (equation (5.7)). The λ_1, hence, is the LOS to the virtual target at T'. V is the speed of the missile. The look angle rate becomes:

$$\dot{\sigma_1} = \dot{\gamma_1} - \dot{\lambda_1} = \dot{\lambda_1} \tag{5.10}$$

This stage continues until the flight path angle equals the LOS angle, which is a condition for the missile velocity being aligned with the LOS. Thus, the switching to the second stage occurs when:

$$\gamma = \lambda \tag{5.11}$$

where γ and λ are the angles in the 3D frame (X, Y, Z). The initial conditions of the first stage, as the X axis is taken along the direction of LOS, e_{LOS_1}, are:

$$\sigma_{1_0} = \gamma_{1_0}; \quad \lambda_{1_0} = 0 \tag{5.12}$$

where the subscript '0' denotes the initial condition.

Following the first stage, the missile enters the second plane. The engagement in the second plane is controlled by a small variation of the TVBPN law, which involves two stages as discussed. This variation is of concern only for very small terminal angles. The lateral acceleration and the time rate of change of flight path angle, in the second plane, are given by:

$$a_{M_2} = N_2V\dot{\lambda_2} + Vb_1; \quad \dot{\gamma_2} = N_2\dot{\lambda_2} + b_1 \tag{5.13}$$

where N_2 is the navigation gain for the second and third stage, on the second plane, λ_2 is the LOS angle in the second plane, and b is the time-varying bias that switches between b_1 and b_2. The subscript '2' represents the variables with respect to the second-plane coordinate system (X_2, Y_2) (equation (5.8)). The look angle rate then becomes:

$$\dot{\sigma_2} = \dot{\gamma_2} - \dot{\lambda_2} = (N_2 - 1)\dot{\lambda_2} + b_1 \tag{5.14}$$

Since initially, the velocity vector is aligned with the LOS and the X axis is along the direction of LOS, e_{LOS_2}, the initial conditions are:

$$\sigma_{2_0} = 0; \quad \lambda_{2_0} = 0; \quad \gamma_{2_0} = 0 \tag{5.15}$$

5.3.1 Variation of the TVBPN law:

For the TVBPN law, initially, the bias $|b_1|$ is less than the bias $|b_2|$. As a result, the bias b_1 is used initially. However, for very small terminal impact angles of around 5° and less, the bias $|b_2|$ is used initially as the bias $|b_1|$ is greater than the bias $|b_2|$. But, for the calculation of the virtual target position, which eliminates a possible jump in the acceleration profile, it is not feasible to calculate the initial b_2 in the second plane. This is because the b_2 depends on the terminal impact angle in the second plane, which is hard to calculate. On the other hand, the initial b_1 doesn't depend on the terminal impact angle, making it easier to estimate.

Hence, a small variation of the TVBPN is used for the second plane of the 3-staged 3D IACG law. The variation ensures that b_1 is always taken as the initial bias. This is done by primarily calculating the terminal impact angle at which the initial $|b_1|$ equals the initial $|b_2|$. From equations (5.1) and (5.3):

$$|b_{1_0}| = |b_{2_0}| \tag{5.16}$$

$$\left|(1 - N)\dot{\lambda} + \frac{1}{\tau_1}(\sigma_{\max} - \sigma)\right| = \left|\frac{B_{\text{ref}} - B(t)}{\tau_2}\right| \tag{5.17}$$

For the initial conditions in the second plane (equation (5.15)), and from equations (2.8), (2.15), and (5.4):

$$\frac{\sigma_{\max}}{\tau_1} = \frac{(1 - N_2)\gamma_L}{\tau_2} \tag{5.18}$$

where γ_L is the terminal impact angle in the second plane for which the magnitude of the biases b_1 and b_2 are equal. Rearranging equation (5.18) gives:

$$\gamma_L = \frac{\sigma_{\max}}{(1-N_2)}\frac{\tau_2}{\tau_1} \tag{5.19}$$

The switching criteria for the variation of TVBPN are given as:

$$b = \begin{cases} \begin{cases} b_1, & |b_2| < |b_1| \\ b_2, & |b_2| \geq |b_1| \end{cases} & if \;\; |\gamma_f| < |\gamma_L| \\ \\ \begin{cases} b_1, & |b_1| < |b_2| \\ b_2, & |b_1| \geq |b_2| \end{cases} & if \;\; |\gamma_f| \geq |\gamma_L| \end{cases} \tag{5.20}$$

where γ_f is the terminal impact angle in the second plane. This variation in the criteria makes sure that the initial bias is always b_1 and that the FOV constraint is considered, all while keeping the lateral acceleration ($|a_M|$) profile continuous.

5.3.2 Calculation of the Virtual Target Position:

The position of the virtual target is calculated on the basis of the requirement that the acceleration must be continuous when the missile goes from the first plane to the second. For the same, the terminal acceleration of the first stage is equated with the initial acceleration of the second stage as:

$$|a_{M_1}(t_{s_1})| = |a_{M_2}(0)| \tag{5.21}$$

where t_{s_1} is the switching time from the first stage to the second. Hence,

$$|2V\dot{\lambda_1}(t_{s_1})| = |N_2V\dot{\lambda_2}(0) + Vb_1(0)| \tag{5.22}$$

As for the PNG of $N = 2$, since the acceleration command remains constant, the initial acceleration and the terminal acceleration in the first plane are the same. The virtual target is at the k^{th} fraction of the initial LOS (r_0). Then, using the initial conditions [(5.12) and (5.15)], and the equations (2.8) and (5.1), we can write (5.22) as:

$$\frac{2V^2 sin(\gamma_{1_0})}{kr_0} = \frac{V\sigma_{\max}}{\tau_1} \tag{5.23}$$

Rearranging (38) gives:

$$k = \frac{2V\tau_1 sin(\gamma_{1_0})}{r_0\sigma_{\max}} \tag{5.24}$$

5.4 Simulations

5.4.1 The TVBPN Guidance Law

The BPNG Law was initially simulated for a constant-speed missile. The speed of the missile is taken as 250 m/s. The initial missile flight path angle was taken as 0°, as is the case for the second plane of the novel 3-Staged 3D IACG Law. PN gain was taken as 3. Time constants, τ_1 and τ_2, were chosen to be 2 and 0.5, respectively. The missile was initially at (0.0) and the stationary target was at $(4000, 0)$. The simulations were carried out for terminal impact angles of 0°, -30°, -90°, -120°, -150°, and -180°. The plots of the obtained results are shown in Figure 5.1.

5.4.2 The 3-Staged 3D IACG Law

5.4.2.1 Varying Impact Conditions

The performance of the proposed guidance law was analyzed by conducting simulations for a constant-speed missile in MATLAB. The missile speed was taken as 50 m/s. The initial location of the missile was $(0, 0, 0)$ and the target location was $(2500, 2500, 2500)$. The initial velocity was along the vector $(1, 1, 0)$. The maximum allowed look angle in the second plane was taken as 45°. Time constants τ_1 and τ_2 were taken as 2 and 0.5, respectively. The impact conditions of the form (Azimuth angle, Elevation Angle) were taken as $(-45^\circ, -45^\circ)$, $(-60^\circ, -30^\circ)$, $(-30^\circ, -60^\circ)$, $(-90^\circ, -45^\circ)$ and $(-179^\circ, -75^\circ)$. The obtained plots are shown in Figure 5.2.

5.4.2.2 Varying Launch Conditions

The proposed guidance law was then simulated for varying launch conditions. The maximum allowed look angle in the second plane was taken as 45°. Time constants τ_1 and τ_2 were taken as 2 and 0.5, respectively. Terminal impact direction was taken as $(1, -1, 1)$. The initial missile flight path conditions or the launch conditions of the form (Azimuth angle, Elevation Angle) were taken as $(-45^\circ, -45^\circ)$, $(-60^\circ, -30^\circ)$, $(-30^\circ, -60^\circ)$, $(-90^\circ, -45^\circ)$ and $(-179^\circ, -75^\circ)$. Other initial conditions were the same as those for the simulations involving varying impact conditions. Results are shown in Figure 5.3.

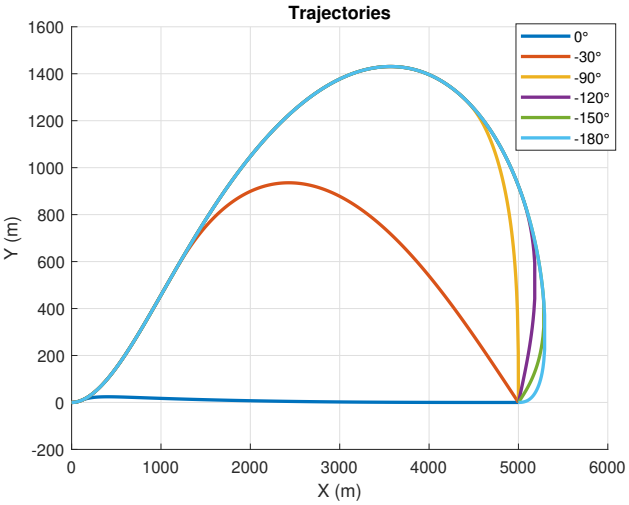

(a)

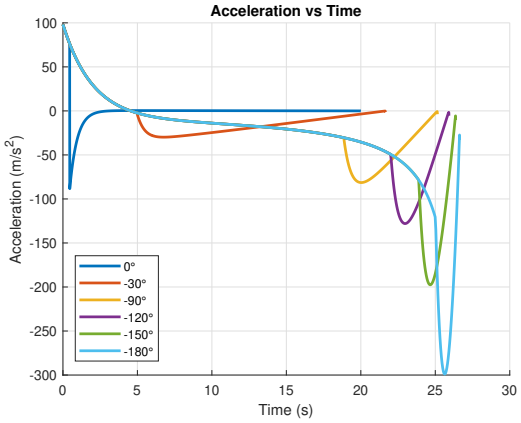

(b)

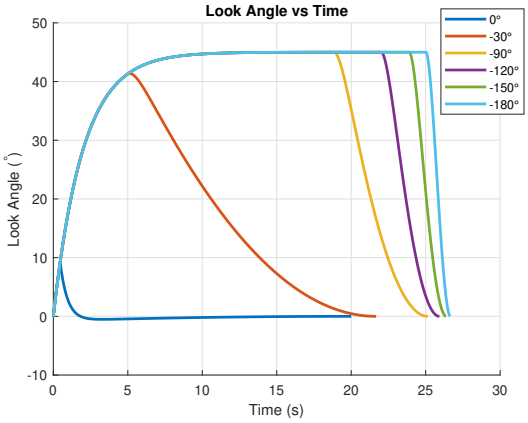

(c)

Figure 5.1: Simulation results of TVBPN Guidance Law

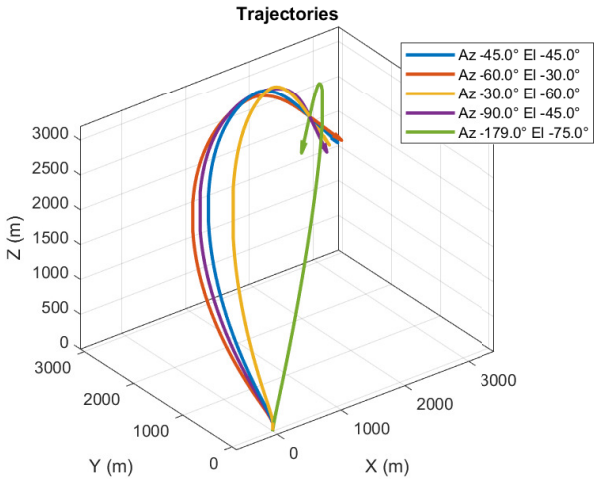

(a)

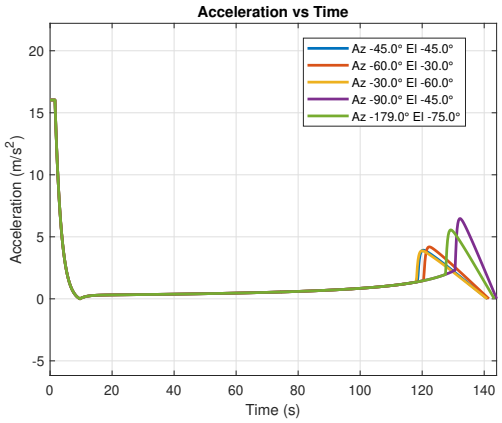

(b)

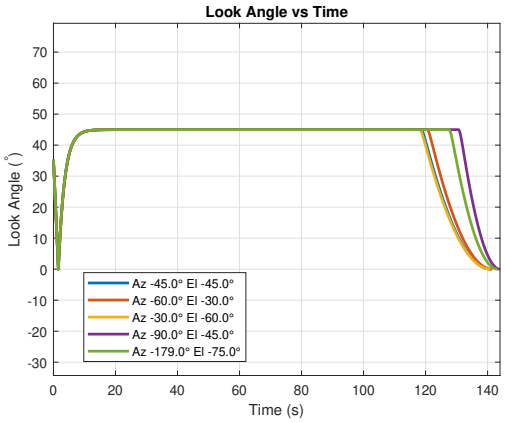

(c)

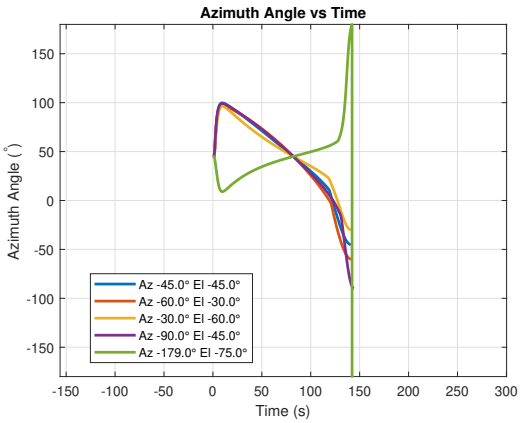

(d)

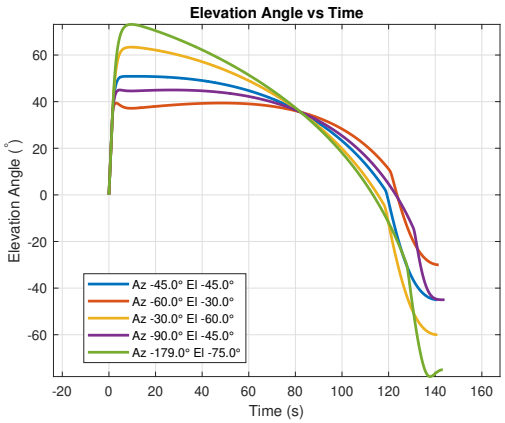

(e)

Figure 5.2: Simulation results of 3-Staged 3D IACG Law - Varying Impact Conditions

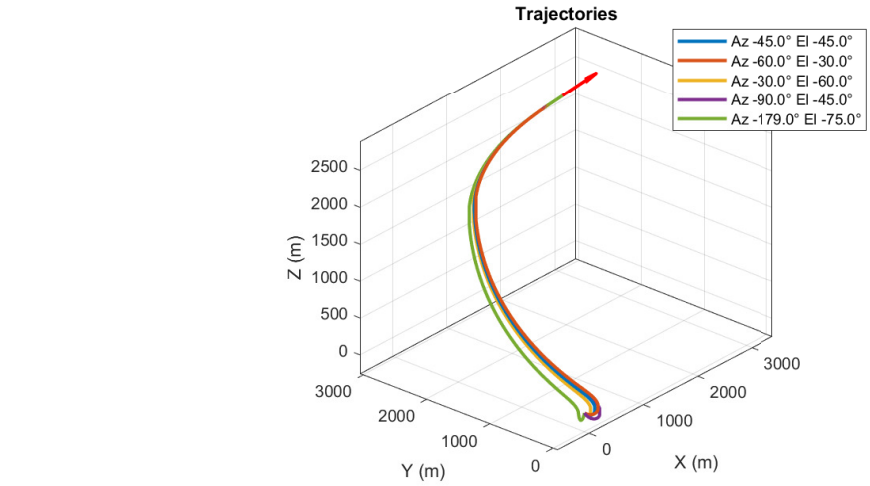

(a)

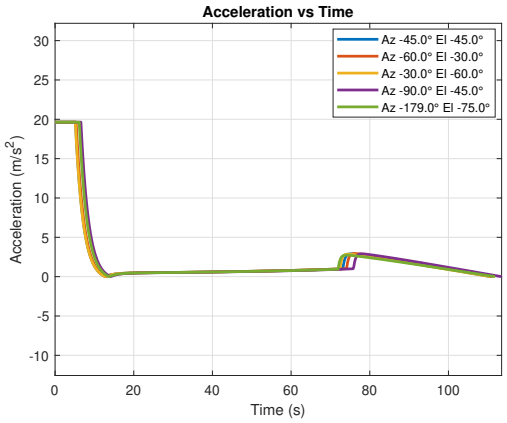

(b)

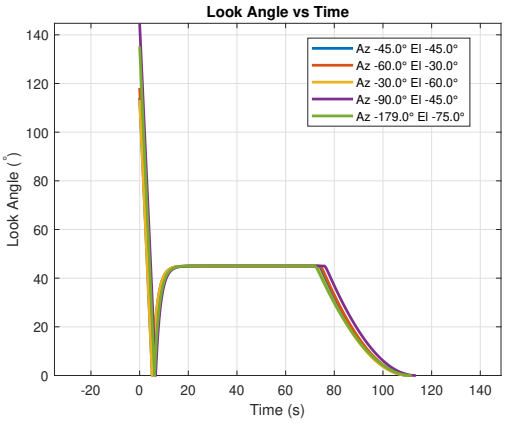

(c)

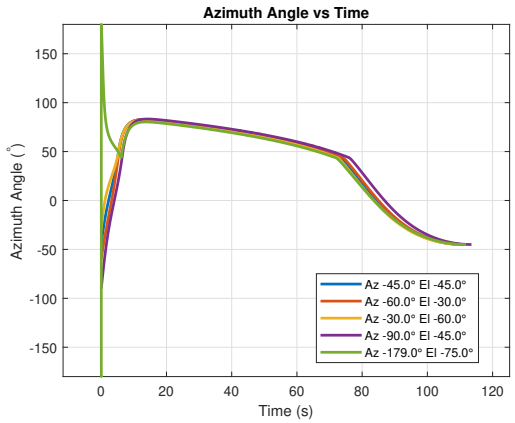

(d)

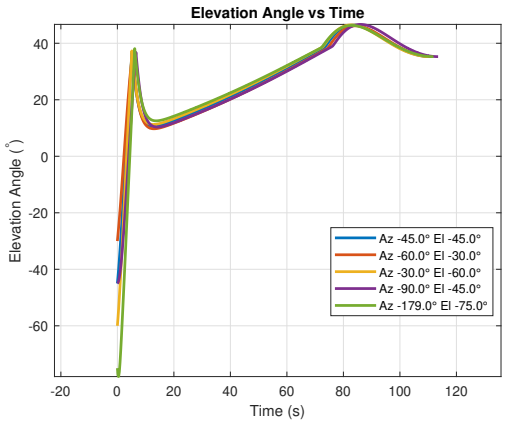

(e)

Figure 5.3: Simulation results of 3-Staged 3D IACG Law - Varying Launch Conditions

5.4.2.3 Comparison Studies

The proposed guidance law was then subjected to comparative simulations with the Non-linear 3D guidance law (21) and the $\mu\alpha CIG3D$ law (23). The missile was considered to be traveling at a constant speed of 50 m/s. The initial location of the missile was $(0, 0, 0)$ and the stationary target location was at $(2500, 2500, 2500)$. The initial velocity was along the vector $(-1, 1, 1)$. Terminal impact azimuth and elevation angles were taken as $-45°$ and $-45°$ respectively. The results of the same have been shown in Figure 5.4.

Furthermore, comparative simulations were conducted for various initial conditions. This time, the terminal impact angles were varied as shown in the comparison table 5.1. The total control efforts and the impact times were calculated and compared.

Method	ψ	ϕ	**Total control effort** (m^2/s^3)	**Impact time (s)**
3-Staged 3D IACG	-45	-45	1928.4	115.0658
$\mu\alpha CIG3D$			2054.2	101.3385
Non Linear 3D			233.8426	143.568
3-Staged 3D IACG	-60	-30	1954.08	115.4691
$\mu\alpha CIG3D$			2099.547	101.5826
Non Linear 3D			234.909	144.8568
3-Staged 3D IACG	-30	-60	1923.86	114.9882
$\mu\alpha CIG3D$			2044.832	101.2837
Non Linear 3D			245.0089	145.0614
3-Staged 3D IACG	-90	-45	2173.956	117.5076
$\mu\alpha CIG3D$			2491.974	102.8204
Non Linear 3D			322.5467	162.400
3-Staged 3D IACG	-135	-60	2299.144	118.1149
$\mu\alpha CIG3D$			2704.926	104.9245
Non Linear 3D			471.6289	188.3434
3-Staged 3D IACG	-180	-75	2089.149	116.9279
$\mu\alpha CIG3D$			2326.876	102.4323
Non Linear 3D			656.4895	215.8023

Table 5.1: Comparison Table

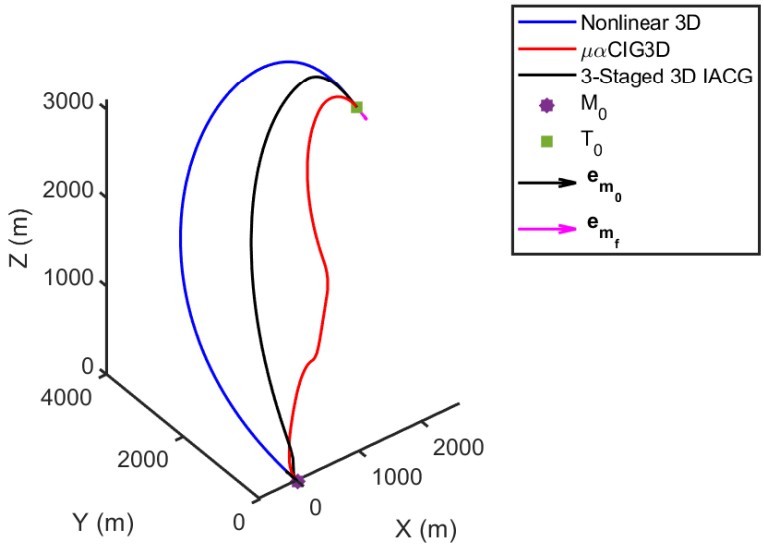

(a)

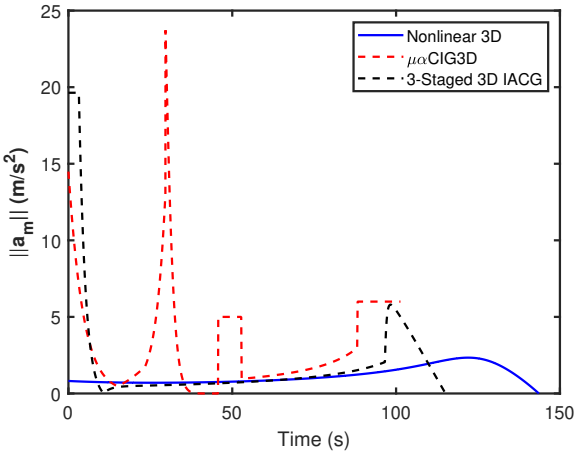

(b)

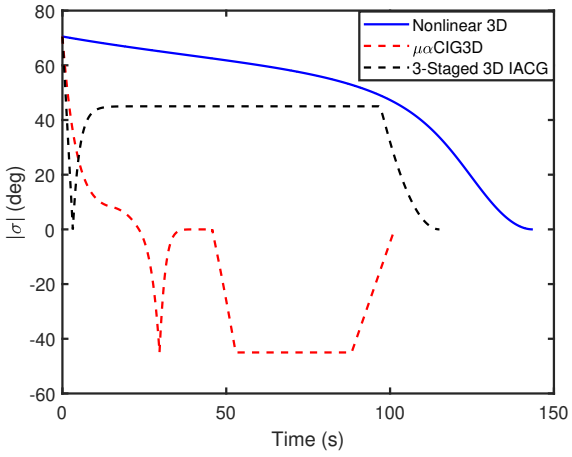

(c)

Figure 5.4: Comparative Simulation results ((a)Trajectories, (b)Acceleration vs Time, (c)Look Angle vs Time)

Chapter 6

Conclusions

6.1 2-Staged PNG to TPG Law

Simulations (Figure 3.2) have shown that the 2-Staged PNG to TPG guidance law (Chapter 3) was successful in achieving all 3D impact directions. Even though this guidance law satisfied the terminal conditions of acceleration and jerk, the missile could not keep the look angle within the lower limits. Still, the look angle profile was bounded. The acceleration profile was continuous everywhere but at the point of plane transition. Since this guidance law used low gains, the impact times for higher impact angles were high. Since these impact times are high, this law wouldn't be practical.

6.2 3-Staged PNG to Triangle TPG Law

The 3-Staged PNG to Triangle TPG law (Chapter 4) successfully achieved all terminal impact directions, as seen in Figure 4.3. This guidance law couldn't keep the look angles under comfortable limits. There were two points of discontinuity of acceleration: one at the plane transition and the other at the triangle centroid. Since, for higher impact angles, the triangle TPG is used for the second plane, the engagement travels under a high look angle, which may not be practical.

6.3 3-Staged 3D IACG Law

Finally, for the 3-Staged 3D IACG Law (Chapter 5), the simulations (Figures 5.2 and 5.3) show that the missile has intercepted the target for all the impact directions and launch conditions. The interception was achieved such that the Look Angles are bounded. There are no discontinuities in the acceleration profile. Even when the impact conditions were

selected to be extremes, the missile intercepted the target comfortably with about zero errors. Hence, this proposed 3-Staged 3D IACG law can achieve all impact angles. The acceleration is also visible to be bounded. Therefore, the initial objective of achieving all 3D impact directions while considering FOV constraints and acceleration continuity is fulfilled successfully.

Comparative simulations (Figure 5.4 and Table 5.1) revealed that the proposed 3-Staged 3D IACG law was superior to the $\mu\alpha CIG3D$ law in terms of the total control effort and the acceleration continuity. The $\mu\alpha CIG3D$ law had multiple discontinuities, whereas the proposed guidance law had none. Even though the Non-Linear 3D law has lower total control effort, the impact time involved is much higher, and the law cannot achieve all impact angles. The proposed guidance law was, thus, superior and was able to achieve the objectives of this study.

Bibliography

[1] Ratnoo, A. and Ghose, D. "Impact angle constrained interception of stationary targets," *Journal of Guidance, Control, and Dynamics*, vol. 31, no. 6, pp. 1817–1822, 2008.

[2] Ratnoo, A. and Ghose, D. "Impact angle constrained guidance against nonstationary nonmaneuvering targets," *Journal of Guidance, Control, and Dynamics*, vol. 33, no. 1, pp. 269–275, 2010.

[3] Ratnoo, A. "Analysis of two-stage proportional navigation with heading constraints," *Journal of Guidance, Control, and Dynamics*, vol. 39, no. 1, pp. 156–164, 2016.

[4] Ranjan, A., Hota, S., and Singh, N. K. "Three-stage proportional navigation for intercepting stationary targets with impact angle constraints," in *Proceedings of the Sixth Indian Control Conference (ICC)*, pp. 379–384, 2019.

[5] Kim, T.-H., Park, B.-G., and Tahk, M.-J. "Bias-shaping method for biased proportional navigation with terminal-angle constraint," *Journal of Guidance, Control, and Dynamics*, vol. 36, no. 6, pp. 1810–1816, 2013.

[6] Park, B.-G., Kim, T.-H., and Tahk, M.-J. "Biased PNG with terminal-angle constraint for intercepting nonmaneuvering targets under physical constraints," *IEEE Transactions on Aerospace and Electronic Systems*, vol. 53, no. 3, pp. 1562–1572, 2017.

[7] Park, B.-G., Kim, T.-H., and Tahk, M.-J. "Optimal impact angle control guidance law considering the seeker's field-of-view limits," *Proceedings of the Institution of Mechanical Engineers, Part G: Journal of Aerospace Engineering*, vol. 227, no. 8, pp. 1347–1364, 2013.

[8] Lee, C.-H., Kim, T.-H., Tahk, M.-J., and Whang, I.-H. "Polynomial guidance laws considering terminal impact angle and acceleration constraints," *IEEE Transactions on Aerospace and Electronic Systems*, vol. 49, no. 1, pp. 74–92, 2013.

[9] Yang, Z., Wang, H., and Lin, D. "Time-varying biased proportional guidance with seeker's field-of-view limit," *International Journal of Aerospace Engineering*, vol. 2016, no. 1, article ID 9272019, 2016.

[10] Erer, K. S., and Tekin, R. "Impact vector guidance," *Journal of Guidance, Control, and Dynamics*, vol. 44, no. 10, pp. 1892–1901, 2021.

[11] Kim, J.-H., Park, S.-S., Park, K.-K., and Ryoo, C.-K. "Quaternion based three-dimensional impact angle control guidance law," *IEEE Transactions on Aerospace and Electronic Systems*, vol. 57, no. 4, pp. 2311–2323, 2021.

[12] Wang, C., Yu, H., Dong, W., and Wang, J. "Three-dimensional impact angle and time control guidance law based on two-stage strategy," *IEEE Transactions on Aerospace and Electronic Systems*, vol. 58, no. 6, pp. 5361–5372, 2022.

[13] Majumder, K., and Kumar, S. R. "Three-dimensional impact angle constrained nonlinear guidance with predefined convergence time," *Nonlinear Dynamics*, vol. 112, no. 12, pp. 9983–10008, 2024.

[14] Nanavati, R. V., Kumar, S. R., and Maity, A. "Lead-angle-based three-dimensional guidance for angle-constrained interception," *Journal of Guidance, Control, and Dynamics*, vol. 44, no. 1, pp. 190–199, 2021.

[15] Zhou, H., Cheng, T., Liu, X., and Chen, W. "Three-dimensional geometric descent guidance with impact angle constraint," *IEEE Access*, vol. 8, pp. 64932–64948, 2020.

[16] Duvvuru, R., Maity, A., and Umakant, J. "Three-dimensional field of view and impact angle constrained guidance with terminal speed maximization," *Aerospace Science and Technology*, vol. 126, article 107552, 2022.

[17] Gu, Z., Kang, H., and Song, S. "Three-dimensional prescribed performance guidance law with field-of-view constraint and feasibility analysis," *International Journal of Aeronautical and Space Sciences*, vol. 25, no. 4, pp. 1536–1553, 2024.

[18] Wang, J., Tao, X., Dong, W., and Wang, C. "Three-dimensional predefined-time impact angle control guidance law with field-of-view limit," *Journal of the Franklin Institute*, vol. 360, no. 12, pp. 7621–7644, 2023.

[19] Wang, J., Ding, X., Chen, Y., Wang, C., and Xin, M. "Field-of-view constrained three-dimensional impact angle control guidance for speed-varying missiles," *IEEE Transactions on Aerospace and Electronic Systems*, vol. 58, no. 5, pp. 3992–4003, 2022.

[20] Han, T., Hu, Q., and Xin, M. "Three-dimensional approach angle guidance under varying velocity and field-of-view limit without using line-of-sight rate," *IEEE Transactions on Systems, Man, and Cybernetics: Systems*, vol. 52, no. 11, pp. 7148–7159, 2022.

[21] Hu, Q., Han, T., and Xin, M. "Analytical solution for nonlinear three-dimensional guidance with impact angle and field-of-view constraints," *IEEE Transactions on Industrial Electronics*, vol. 68, no. 4, pp. 3423–3433, 2020.

[22] Surve, P., Maity, A., and Kumar, S. R. "Polynomial shaping based three-dimensional impact angle and field-of-view constrained guidance," *Aerospace Science and Technology*, vol. 147, article 109018, 2024.

[23] Ghosh, S., Yakimenko, O. A., Davis, D. T., and Chung, T. H. "Unmanned aerial vehicle guidance for an all-aspect approach to a stationary point," *Journal of Guidance, Control, and Dynamics*, vol. 40, no. 11, pp. 2871–2888, 2017.